Cellular Mechanism of HCO3- and Cl- Transport in Insect Salt Gland

K. Strange* and J.E. Phillips
Department of Zoology, University of British Columbia, Vancouver, British Columbia, V6T 2A9, Canada

Summary. Active HCO_3^- secretion in the anterior rectal salt gland of the mosquito larva, *Aedes dorsalis*, is mediated by a 1 : 1 Cl^-/HCO_3^- exchanger. The cellular mechanisms of HCO_3^- and Cl^- transport are examined using ion- and voltage-sensitive microelectrodes in conjunction with a microperfused preparation which allowed rapid saline changes. Addition of DIDS or acetazolamide to, or removal of CO_2 and HCO_3^- from, the serosal bath caused large (20 to 50 mV) hyperpolarizations of apical membrane potential (V_a) and had little effect on basolateral potential (V_{bl}). Changes in luminal Cl^- concentration altered V_a in a rapid, linear manner with a slope of 42.2 mV/decalog $a_{Cl^-}^i$. Intracellular Cl^- activity was 23.5 mM and was approximately 10 mM lower than that predicted for a passive distribution across the apical membrane. Changes in serosal Cl^- concentration had no effect on V_{bl}, indicating an electrically silent basolateral Cl^- exit step. Intracellular pH in anterior rectal cells was 7.67 and the calculated $a_{HCO_3}^i$ was 14.4 mM. These results show that under control conditions HCO_3 enters the anterior rectal cell by an active mechanism against an electrochemical gradient of 77.1 mV and exits the cell at the apical membrane down a favorable electrochemical gradient of 27.6 mV. A tentative cellular model is proposed in which Cl enters the apical membrane of the anterior rectal cells by passive, electrodiffusive movement through a Cl^--selective channel, and HCO_3 exits the cell by an active or passive electrogenic transport mechanism. The electrically silent nature of basolateral Cl^- exit and HCO_3 entry, and the effects of serosal addition of the Cl^-/HCO_3 exchange inhibitor, DIDS, on $J_{net}^{CO_2}$ and transepithelial potential (V_{te}) suggest strongly that the basolateral membrane is the site of a direct coupling between Cl and HCO_3 movements.

Key Words bicarbonate transport · insect rectum · epithelia · chloride absorption · intracellular Cl^- · pH

Introduction

The larvae of a number of species of mosquitoes can survive in environments ranging from distilled water to water several times the concentration of seawater. In saline environments hemolymph ionic and osmotic concentrations are maintained well below those of the surrounding medium (reviewed by Phillips, Bradley & Maddrell, 1978). This hyporegulation is achieved primarily by excretion of a hyperosmotic urine with ionic concentrations and ratios similar to those found in the animals' external environment. Studies by Bradley and Phillips (1975) demonstrated clearly that the rectum was the site of hyperosmotic urine formation and that this urine was produced by direct secretion of a hyperosmotic fluid into the rectal lumen. Thus, the rectum or rectal salt gland functions in a manner analogous to the salt glands of birds and reptiles.

The rectal salt gland of saltwater mosquito larva is composed of two morphologically distinct segments referred to as the anterior and posterior segments. Each segment of the salt gland is composed of a single ultrastructurally distinct cell type and the two segments are linked together by a single row of small, relatively indistinct junctional cells (Meredith & Phillips, 1973). Microcannulation studies by Strange, Phillips and Quamme (1984) demonstrated that the posterior segment secretes 75% and the anterior segment 25% of the fluid secreted by the whole gland. Furthermore, these investigators showed that fluid secretion in the gland appeared to be driven by Na^+ and Cl^- transport. Removal of Na^+ or Cl^- from the medium bathing the glands inhibited fluid secretion by 57 to 92%. Glands bathed in HCO_3^--free salines produced strongly hyperosmotic secretions at near normal rates containing almost pure NaCl. Subsequently, these investigators suggested that the salt gland normally secretes a NaCl-rich fluid into the lumen and that the composition of this fluid is modified by ion exchange and reabsorption processes which are dependent upon the osmotic regulatory needs of the animal.

In addition to surviving in strongly hypersaline waters certain species of mosquito larvae can in-

---

Present address: Laboratory of Kidney and Electrolyte Metabolism, National Institutes of Health, Bldg. 10, Room 6N319, Bethesda, MD 20205.

habit inland saline ponds with waters composed primarily of high concentrations of $NaHCO_3$ and Na_2CO_3, $MgSO_4$ or Na_2SO_4 (e.g., Scudder, 1969). Strange, Phillips and Quamme (1982) recently showed that under laboratory conditions larvae of the mosquito *Aedes dorsalis* can survive and develop normally in saline media with pH values up to 10.5, HCO_3^- concentrations up to 250 mM, or CO_3^{2-} concentrations up to 100 mM. Despite ingestion of these alkaline media at rates equivalent to 130% of larval body weight per day, these insects regulate hemolymph pH (7.55 to 7.70) and HCO_3^- concentrations (8.0 to 18.5 mM) within narrow physiological limits (Strange et al., 1982). Micropuncture and microcannulation studies of the rectal salt gland demonstrated that this organ was an important site of pH and HCO_3^- regulation. Microcannulated salt glands secrete a strongly hyperosmotic fluid containing 402 mM HCO_3^- and 41 mM CO_3^{2-} at a rate of 38 nl $\cdot$ hr^{-1}. Lumen-to-bath HCO_3^- and CO_3^{2-} gradients of 21 : 1 and 241 : 1, respectively, are generated by the salt gland epithelium against a V_{te} of -25 mV (lumen negative), demonstrating clearly the active nature of HCO_3^- secretion (Strange et al., 1982).

The mechanisms of active HCO_3^- transport have been recently studied using an *in vitro* microperfused rectal salt gland preparation (Strange & Phillips, 1984). Net total CO_2 transport ($J_{net}^{CO_2}$) as measured by microcalorimetry in perfused salt glands is unaffected by bilateral Na^+ or K^+ and serosal Cl^- substitutions, or by serosal addition of 1.0 mM ouabain, 2.0 mM amiloride or 0.5 mM SITS. Removal of luminal Cl^- inhibited $J_{net}^{CO_2}$ by 80%, while serosal addition of 1.0 mM acetazolamide or 0.5 mM DIDS inhibited $J_{net}^{CO_2}$ by 80% and 40%, respectively.

Perfusion of the anterior and posterior rectal segments demonstrated clearly that the anterior rectum is the site of CO_2 secretion in the microperfused salt gland (Strange et al., 1984). Net Cl^- absorption in the anterior segment, as measured by electron microprobe analysis, is equivalent to the rate of CO_2 secretion. In addition, Cl^- reabsorption in the anterior segment is completely inhibited by bilaterally replacing CO_2 and HCO_3^- with a phosphate or HEPES-buffered saline (Strange et al., 1984). These data provide strong quantitative evidence for the presence of a 1 : 1 Cl^-/HCO_3^- exchange mechanism located in the anterior rectal salt gland segment and indicate that the anterior segment is at least one site where modification of the primary NaCl-rich rectal secretion can occur.

In the present investigation, the cellular mechanisms of anterior salt gland HCO_3^- and Cl^- transport were examined using ion and voltage-selective microelectrodes in conjunction with a microperfused

anterior segment preparation which allowed complete changes in serosal and mucosal saline composition to be made in <5 to 10 sec.

Materials and Methods

ANIMALS

Larvae were reared in a low alkalinity rearing medium and the adult colony maintained as described previously (Strange et al., 1982). Three days after hatching, larvae were transferred to 250 mM HCO_3^- medium containing (in mM): 361.5 Na^+, 2.5 K^+, 0.03 Ca^{2+}, 0.50 Mg^{2+}, 39.6 Cl^-, 10.0 SO_4^2 , 250 HCO_3^-, 29.0 CO_3^{2-}, pH 8.9. All experiments were conducted at room temperature (21 to 24°C) using fourth instar larvae acclimated to this medium for three to six days.

MICROPERFUSION SYSTEM

Collection pipets were constructed as described by Strange and Phillips (1984). Perfusion pipets were fabricated by sealing a small glass cannula (o.d. 50 to 60 μm, i.d. 35 to 40 μm, tip opening 20 to 25 μm) with a long column of epoxy into a glass pipet pulled from flint glass tubing (o.d. 1.0 mm, i.d. 0.8 mm; Drummond Glass Co., Broomall, Pa.). The epoxy seal was waterproofed and electrically insulated using cured Sylgard® 184 resin (Dow Corning). Bath chambers were constructed from molded Sylgard® 184 resin and were similar to those described by Strange and Phillips (1984) except that two superfusion inlets were positioned on either side of the salt gland preparation and the total chamber volume was reduced to approximately 0.6 ml.

Rectal salt glands were dissected as described previously (Strange & Phillips, 1984). In these studies the anterior segment alone was perfused by cannulating the midgut and ileum with a perfusion pipet and the anal canal and posterior segment with a collection pipet (Fig. 1). Two or three ligatures with a diameter of ca. 10 μm (see Strange & Phillips, 1984) were tied around the ileum and anal canal to ligate these pipets into place. An additional one or two ligatures were tied one cell row or approximately 50 μm posterior to the junctional region to isolate the anterior salt gland. The transepithelial potential in perfused anterior segments was allowed to stabilize after set-up for 30 to 40 min before experiments were begun.

BATH AND LUMINAL SOLUTION CHANGES

The bath chamber was normally superfused by gravity at a rate of 3 to 5 ml $\cdot$ min^{-1}. Rapid changes (<5 sec) in bath composition were made by using a 6-way rotary valve (Altex, Rainin Instrument Co. Inc., Woburn, Mass.) and by increasing the rate of superfusion to 20 to 30 ml $\cdot$ min^{-1}. While this high superfusion rate tended to cause a small amount of mechanical disturbance to the preparation, it was nevertheless possible to maintain a high number of stable microelectrode impalements during these solution changes (see Results). Bathing salines were delivered to the rotary valve and bath chamber through polyethylene tubing (PE 240).

Rapid changes in luminal solution composition were made using a double pipet arrangement shown schematically in Fig. 1
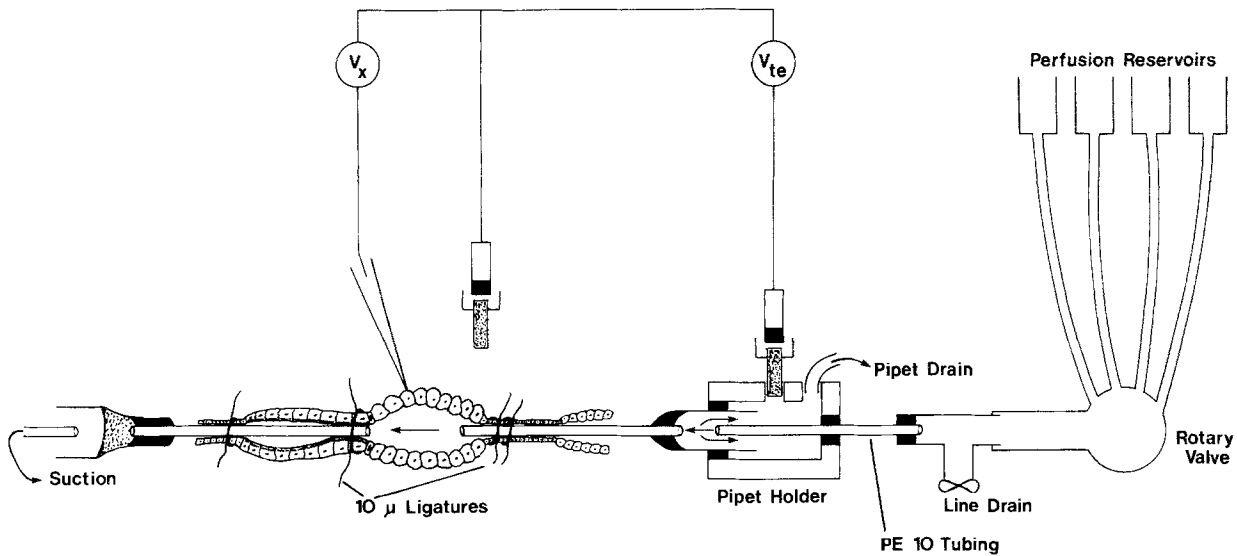
Fig. 1. Schematic diagram of microperfused anterior rectal salt gland segment and double perfusion pipet arrangement for rapid changes in luminal salines (i.e. 5 to 10 S)

and described by Strange (1983). The perfusion rate through the PE 10 tubing was approximately 0.6 ml · min⁻¹ and the bulk of perfusion solution flowed out the pipet (Fig. 1) to a waste container. An adjustable pinch clamp on the line draining the pipet holder allowed adjustment of luminal perfusion to rates of 150 to 250 nl · min⁻¹. Changes in luminal fluid composition were made by choosing one of four perfusates using the rotary valve and then opening the line drain for 3 to 4 sec to flush the perfusion line. When the drain was closed, a new perfusate almost instantaneously began flushing the perfusion pipet and salt gland lumen. The total time for a complete luminal solution change was <10 sec. Although this procedure necessarily caused very small luminal pressure transients when the line drain was opened and closed, it was possible to maintain an acceptable number of microelectrode impalements by impaling cells close to the perfusion and collection pipets.

Both the perfusion and collection pipet holders were mounted on Narishige micromanipulators (Model MM-3, Narishige Instrument Laboratories, Tokyo). Perfusates collecting in the collection pipet were continuously drawn off to waste by vacuum suction through a glass micropipet attached to a length of polyethylene tubing (PE 100; *see* Fig. 1).

ELECTRICAL MEASUREMENTS

Transepithelial potential was measured with reference to the bathing saline using calomel half-cells and a Keithley Model 616 digital electrometer (Keithley Instruments Inc., Cleveland, Ohio). The calomel half-cells made contact via 3 M KCl—4% agar bridges with the bath saline through a port in the bath chamber and with the perfusion saline through a gasket-sealed port on the perfusion pipet holder (Fig. 1). Changes in agar bridge junction potentials which occurred during solution changes were measured separately against a grounded calomel half-cell: data were corrected only when junction potentials were ≥1.0 mV. Transepithelial potential was recorded continuously on one channel of

a 2-channel chart recorder (Model 7402A, Hewlett-Packard, San Diego, Calif.).

Voltage-sensitive microelectrodes were pulled on a Narishige vertical pipet puller (Model PE 2, Narishige) from capillary glass (1.0 mm o.d., Frederick Haer and Co., Brunswick, Maine). These microelectrodes had resistances of either 10 to 12 MΩ or 30 to 50 MΩ. The lower resistance microelectrodes were used in later studies since they provided stabler impalements and virtually eliminated the problem of changing tip potentials which occasionally occurred during and after cell puncture. Both high and low resistance microelectrodes gave the same values for V_{bl}, were filled with 0.5 or 3.0 M KCl, and had tip potentials <5.0 mV. Voltage output from these electrodes was measured using a Model M701 Microprobe System (WP Instruments, New Haven, Conn.) or a differential electrometer (Model FD 223, WP Instruments), were monitored on a storage oscilloscope (Model D15, Tektronix, Beaverton, Oregon) and recorded continuously on one channel of a 2-channel chart recorder (Model 7402A, Hewlett-Packard). Apical membrane potential was determined simply as the difference between V_{bl} and V_{te}.

In our hands, we could not construct reliably double-barrelled liquid ion-exchanger microelectrodes (*see* Fujimoto & Kubota, 1976) with tip diameters <1.0 μm. Microelectrodes with tip diameters this large were ineffective in impaling anterior rectal cells probably because of the presence of a rather thick basement membrane in this tissue (Meredith & Phillips, 1973). Therefore, it was necessary to use single-barrelled ion-selective microelectrodes which had tip diameters that consistently measured ≤0.5 μm. These electrodes were pulled from acid-washed capillary glass on a Narishige vertical pipet puller, silanized by dipping their tips for 10 to 12 sec into a 0.2% solution (vol/vol) of Dow Corning 1107 silicone oil in acetone (Aristar, BDH Chemicals Ltd., Poole, England) and baked at approximately 300°C on a hotplate for 15 to 25 min.

Chloride-sensitive microelectrodes were constructed by injecting a small column of Cl⁻-exchange resin (Orion 92-17102, Orion Research) into the electrode shank with a syringe and

Table 1. Composition of physiological salines[a]

Component (mM)	Bathing salines			Perfusion salines	
	Control	CO_2-free (HEPES)	CO_2-free (Glycodiazine)	Control	CO_2-free (HEPES)
Na^+	189.5	189.5	189.5	148.5	148.5
K^+	9	9	9	50	50
Mg^{2+}	4	4	4	4	4
Ca^{2+}	4	4	4	4	4
Cl^-	39	39	39	164	164
HCO_3^-	18.5	—	—	18.5	—
CO_3^{2-}	—	—	—	—	—
SO_4^{2-}	4.5	4.5	4.5	5	5
Isethionate$^-$	125	141.5	125	—	16
HEPES	—	5	—	—	5
Glycodiazine$^-$	—	—	18.5	—	—
pH	7.7	7.7	7.7	7.7	7.7
CO_2 (%)	2	0		2	0
O_2 (%)	98	100	100	98	100
Lissamine Green (%)	—	—	—	0.05	0.05

[a] All salines also contained the following (in mM): proline 20, alanine 5, glycine 3, glutamine 4, succinate 2.4, citrate 2.4, glucose 10.

drawn-out polyethylene tubing. The microelectrodes were placed tip down into 0.5 M KCl overnight and the resin allowed to fill the electrode tip. The following day electrodes were back-filled with 0.5 M KCl and bevelled by jet stream abrasion (Ogden, Citron & Pierantoni, 1978) at a 45° angle for approximately 30 sec. Chloride-sensitive electrodes were usually functional for 3 to 4 days.

Hydrogen-sensitive microelectrodes were constructed in a similar manner using a H^+-exchange resin which was a generous gift from Dr. W. Simon (see Ammann et al., 1981). This resin was stored continuously under 100% CO_2. After filling the electrode shank with a small column of the resin, electrodes were placed tip down in a pH 7.0 buffer and left overnight in a dessicator under 100% CO_2. The microelectrodes were back-filled the next day with pH 7.0 buffer (see Ammann, et al., 1981) and bevelled as described above. The H^+-exchange microelectrodes were usually only functional for 1 day.

The voltage outputs of ion-sensitive microelectrodes were measured using a differential electrometer with $10^{15}\Omega$ input resistance (Model FD 223, WP Instruments), and the signal was filtered before recording using a low-pass filter. The Cl^--sensitive microelectrodes were calibrated in 3 to 4 solutions containing 1, 5, 50 or 150 mM KCl. Ion activities were calculated using the Debye-Hückel equation (Robinson & Stokes, 1965) and ion size parameters from Kielland (1937). These electrodes had slopes of 50 to 60 mV/decalog Cl^- activity and selectivities for Cl^- over HCO_3^- ranging between 3 and 5. Intracellular ion activity coefficients were assumed to be the same as those in free solution (i.e. 0.73).

Hydrogen-sensitive microelectrodes were calibrated in 3 buffers (pH 6.4 to 8.3) of constant ionic strength similar to the bathing saline and had slopes of 55 to 60 mV/pH unit. The pH of calibration buffers was determined before each experiment using a Radiometer Model 27 pH meter (Radiometer, Copenhagen) and a Radiometer pH electrode calibrated with Radiometer buffers.

As described previously (Ammann et al., 1981), these H^+-exchanger microelectrodes showed negligible sensitivities to Na^+ or K^+ in concentrations up to 100 mM within the pH range of 6.4 to 8.3. Both H^+- and Cl^--sensitive microelectrodes had resistances of $10^{11}\Omega$ and full response times to step changes in solution of <5 to 8 sec.

MICROELECTRODE IMPALEMENTS

The perfused anterior rectal salt gland was viewed through a dissecting microscope (Zeiss, Jena, East Germany) and illuminated from above by fiber optics (Intralux Model 150 H, Volpi AG, Urdorf, Switzerland). Electrodes were advanced manually at an angle of 45 to 60° to the cell surface using a Leitz micromanipulator (Wetzlar, West Germany) until the microelectrode tip just began to touch the cell membrane. The microelectrode was allowed to 'rub' against the cell membrane for approximately 20 sec and the cell was then impaled by tapping the table gently. In early fourth instar larvae it was possible to remotely advance microelectrodes directly into cells using a hydraulic microdrive (Model MO-8, Narishige).

Acceptable cellular impalements were characterized by an abrupt, monotonic change in microelectrode voltage, a potential which remained stable for at least 1 min, and a return of the microelectrode voltage to within ±2.0 mV of baseline after the electrode was withdrawn from the cell.

SALINES

The composition of various bathing and perfusion salines used throughout this study are shown in Table 1. The control bathing saline was based on measured hemolymph ionic, osmotic and free amino acid concentrations (Strange et al., 1982) while the

Table 2. Calculated Cl and HCO_3 electrochemical gradients for apical and baolateral cell membranes bathed by control salines[a]

Ion	a_i (mM)	V_a (mV)	V_{bl} (mV)	$\Delta\bar{\mu}_{ih}^{a}$ (mV)	$\Delta\bar{\mu}_{ih}^{bl}$ (mV)
Cl	23.5 ± 1.4	−30.8 ± 1.1	−76.6 ± 0.2	−10.7 ± 2.2	71.7
HCO_3	14.4 ± 0.7	−27.3 ± 0.5	−76.2 ± 0.2	27.6 ± 1.3	77.1

[a] Net Cl flux is from lumen to bath and net CO_2 flux is from bath to lumen (Strange et al., 1984). Negative signs indicate a gradient favorable for movement of the ion into the cell. Bicarbonate activity was calculated using the measured pH_c (see Results; $n = 23–39$ impalements on 4–7 preparations).

control perfusates resembled larval Malpighian tubule fluid which normally flows into the rectum (Phillips & Maddrell, 1974). Note that the large anion deficit observed in larval hemolymph (Strange et al., 1982) was simulated in the bathing saline with sodium isethionate (Table 1). Concentrations of Na^-, K^+ and Cl^- were varied in bath and perfusion salines by replacing these ions with $choline^+$, Na^+ or $isethionate^-$, respectively (see Results). Glycodiazine (sodium glymidine) was a generous gift from Mr. H. Wehner (Pentagone Labs Ltd., Vaudreuil, Quebec).

Salines containing acetazolamide (Sigma Chemical Co., St. Louis, Mo.) and DIDS (4-4'-diisothiocyano-2-2'disulfonic acid, Sigma) were made up fresh before each experiment. DIDS was dissolved in amino acid-free saline (replaced with sucrose) since this compound reacts with free amino groups. Preparation of DIDS saline was carried out in a darkened room and the bath superfusion reservoir and lines were wrapped in foil. All tissues were exposed to DIDS for 1 hr in complete darkness.

Results

MEMBRANE POTENTIALS AND INTRACELLULAR ION ACTIVITIES

Mean control values for V_{te} (lumen negative), V_{bl} and V_a (cell negative) were −45.5 ± 0.5, −76.6 ± 0.2 and −30.1 ± 0.4 mV (±SE, $n = 150$ impalements on 39 preparations), respectively. Measurements of V_{bl} showed very little variation between individual cells and individual anterior segment preparations (see Strange, 1983). Basolateral membrane potential measurements were remarkably stable and it was often possible to maintain impalements with voltage electrodes for at least 60 to 90 min. In addition, any given preparation could be repeatedly impaled with voltage microelectrodes with no apparent detrimental effects to the tissue as indicated by very stable transepithelial potentials which changed by no more than ±3.0 mV over the course of a normal 6- to 8-hr experiment. Stable impalements and tissue viability are most likely facilitated by the large size of anterior rectal cells (30 to 40 μm in diameter, 30 to 40 μm long) and the extensive infolding of the basal membrane, which greatly increases membrane surface area (see Meredith & Phillips, 1973).

Since single-barrelled ion-sensitive microelectrodes were used in these studies, V_{bl} in any given preparation was determined at the beginning or end of an experiment and this value subtracted from the observed voltage outputs from either the H^+- or Cl^--sensitive microelectrodes. Mean intracellular pH (pH_c) and Cl^- activity (a_{Cl}^c-)[1] for preparations bathed and perfused with control salines were 7.67 ± 0.03 (± SE, $n = 39$ cells, 4 preparations) and 23.5 ± 1.4 mM (± SE, $n = 23$ cells, 7 preparations; Table 2), respectively, and varied little between individual cells (Strange, 1983).

As with the voltage microelectrodes discussed above, cells could be repeatedly impaled with H^+-sensitive microelectrodes with no apparent deleterious effects to the tissue. The results obtained with Cl^--sensitive electrodes, however, were considerably different. In general, it was possible to make only 5 or 6 attempts at impalements, successful or unsuccessful, on any given preparation before V_{te} would start to rapidly depolarize. Since the problem never occurred with voltage- or H^+-sensitive microelectrodes, which had the same tip dimensions as Cl^--electrodes, the only likely explanation is a direct effect of the Cl^--exchange resin on the tissue itself. This effect could be the result of resin toxicity to cellular metabolism or intriguingly, to a

---

[1] It should be noted at this time that isethionate was used in the serosal saline to simulate the anion deficit observed in larval hemolymph (Strange et al., 1982; Table 1). Generally, gluconate is used as the anion substitute of choice in experiments in which a_{Cl}^c- is measured since Cl^- resins tend to be less sensitive to this compound than most other anion substitutes. In experiments in which gluconate replaced serosal isethionate, however, V_{te} hyperpolarized by approximately 10 to 15 mV and exhibited a continual oscillation of approximately ±5.0 mV (data not shown). This observation is consistent with the fact that gluconate is generally more permeable than Cl^- or many other anion substitutes in certain cells and tissues (see for example, Brown & Saunders, 1977).

direct effect of the resin on electrogenic HCO_3^- transport or apical Cl^- conductance (*see below*). Any preparation which displayed this rapidly depolarizing V_{te} or had a V_{te} which dropped below -40 mV was immediately discarded.
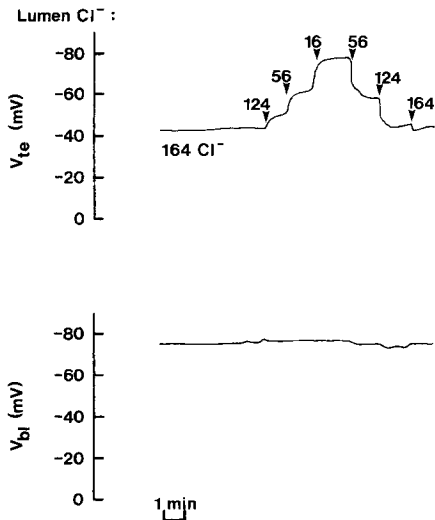

Fig. 2. Effects of rapid changes in luminal Cl^- concentration on V_{te} and V_{bl}. Similar experiments were conducted on a total of 11 separate anterior segment preparations
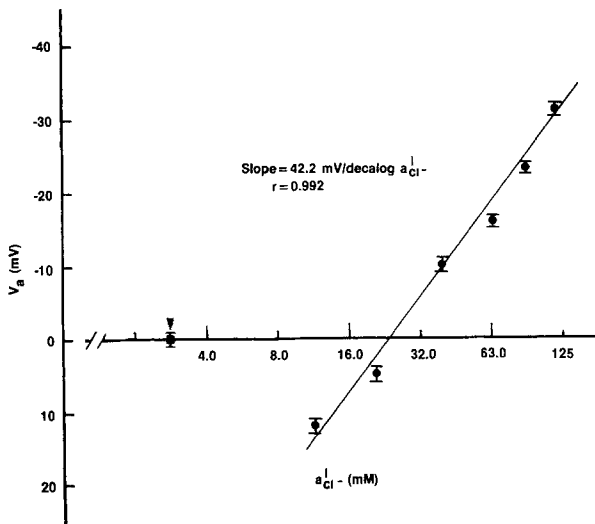

Fig. 3. Relationship between the log of the luminal Cl^- activity ($a_{Cl^-}^l$) and V_a. Each point is the mean $\pm$ SE of 9 to 17 impalements obtained from at least two separate anterior segment preparations. A total of 11 anterior segment preparations were used in these studies. The straight line drawn through the points was determined using the least-squares method of linear regression. The point at the arrow is the value of V_a in the presence of 4 mM luminal Cl^- concentration (*see* Results). The horizontal axis is a log scale of luminal Cl^- activity

MEMBRANE CONDUCTIVE PROPERTIES

Data in Fig. 2 show that rapid decreases in luminal Cl^- concentration cause a rapid, step-wise hyperpolarization of V_{te}. Simultaneous measurements of V_{bl} indicated that these potential changes were located almost entirely at the apical membrane (Fig. 2). The relationship between the logarithm of the luminal Cl^- activity ($a_{Cl^-}^l$) and V_a was found to be linear between Cl^- concentrations of 16 to 164 mM (Fig. 3). The slope of the line for experiments conducted on 11 different preparations was 42.2 mV/decalog $a_{Cl^-}^l$ and the correlation coefficient was 0.992. Chloride concentrations below 16.0 mM caused a repolarization of V_a. At a luminal Cl^- concentration of 4.0 mM, mean V_a was 0.01 ± 1.1 mV ($\pm$ SE; $n = 17$ impalements, 4 preparations; *see* Fig. 3). Mean V_a in the presence of Cl^--free mucosal saline was 0.2 ± 1.1 mV ($\pm$ SE; $n = 5$ impalements, 1 preparation). Rapid changes in luminal Na^+ or K^+ concentration had virtually no effect on V_{te} and V_{bl}, and hence on
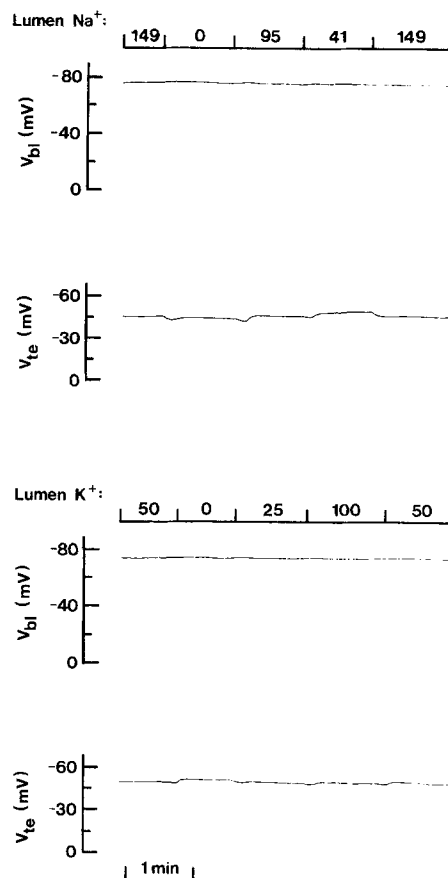

Fig. 4. Effects of luminal Na^+ or K^+ substitutions on V_{te} and V_{bl}. A total of four to five similar experiments were conducted on two separate anterior segment preparations for either the Na^+ or K^+ substitution studies

V_a, indicating an extremely low cation conductance of the apical membrane and paracellular shunts (Fig. 4).

The anterior rectal cell V_{bl} appears to be primarily a K^+ diffusion potential. Changes in serosal K^+ concentration alter V_{bl} in a rapid, linear fashion (Fig. 5). The slope of the relationship between V_{bl} and serosal K^+ activity (a_{K^+}) was 54.2 mV/decalog a_{K^+} with a correlation coefficient of 0.9999 (Fig. 5). Decreases in serosal Na^+ concentration from 189.5 to 165.5 mM had only a small depolarizing effect on V_{bl} (mean ± SE; depolarization = 0.6 ± 0.1 mV; n = 4). Changes in serosal Cl^- concentration from a control value of 39 mM to values of 5, 100 or 164 mM had little effect on V_{bl} (Fig. 6) and V_{te} (data not shown).

The experiments summarized in Fig. 7 suggested that HCO_3^- transport in the anterior rectal

salt gland was electrogenic in nature. Rapid addition of 1.0 mM acetazolamide to the bath, which inhibits $J_{net}^{CO_2}$ in this tissue (Strange & Phillips, 1984), caused a large depolarization of V_{te} (Fig. 7). After a 60-min exposure to acetazolamide, V_{te} had stabilized at a new value of -7.3 ± 3.9 mV (mean ± SE, n = 5). Removal of acetazolamide from the bathing saline caused V_{te} to return to control values within 30 min (Strange, 1983).

The effects of 0.5 mM serosal DIDS on V_{te} are shown in Fig. 7. Tissues were initially exposed to amino acid-free bathing saline (see Materials and Methods) for 60 min and then returned to control saline for 30 min before addition of 0.5 mM DIDS to the bath. In amino acid-free bathing salines, V_{te} hyperpolarized by 8 to 10 mV and then returned to control values in control salines (Strange, 1983). Exposure of the salt gland to serosal DIDS inhibited $J_{net}^{CO_2}$ (Strange & Phillips, 1984) and caused a depolarization of V_{te} (Fig. 7). The time course of this depolarization varied considerably between individual preparations and was complicated by the hyperpolarizing effects of the amino acid-free saline. In addition, V_{te} was not stable after exposure to DIDS for 60 min but usually continued to decline rapidly. Nevertheless, the mean V_{te} of -25.8 ± 3.5 mV (± SE, n = 4) at this time was significantly different (0.0005 < P < 0.01) from the control value of -44.1 ± 0.8 mV (± SE, n = 4). In 3 of the preparations, V_{te}
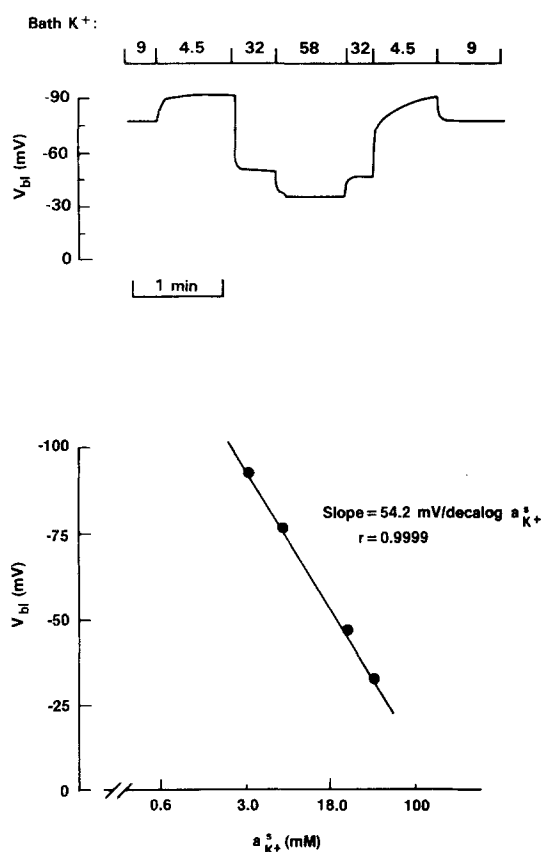

Fig. 5. Effects of rapid changes in serosal K^+ concentration on V_{bl} (upper panel). The relationship between the log of the serosal K^+ activity and V_{bl} is shown in the lower panel. Each point is the mean ± SE of 10 to 13 impalements obtained from four separate anterior segment preparations. The straight line drawn through the points was determined using the least-squares method of linear regression. In all cases the SE bar was smaller than the size of the actual point. The horizontal axis is a log scale of serosal K^+ activity
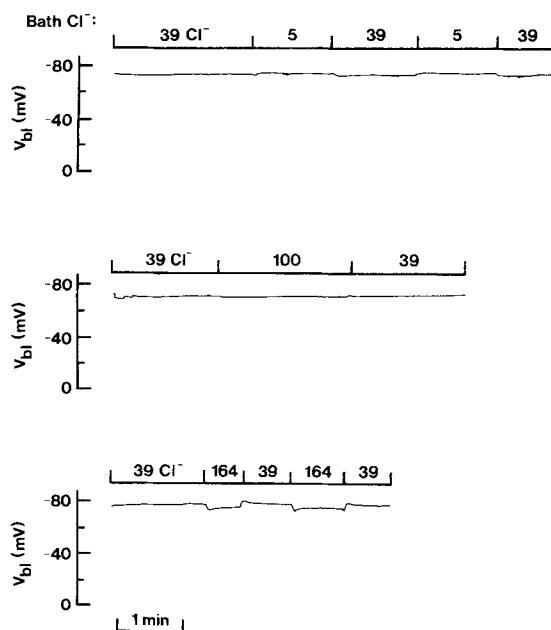

Fig. 6. Effects of rapid changes in serosal Cl^- concentration on V_{bl}. Each trace is the result from an experiment conducted on a separate anterior segment preparation. A total of 8 to 15 similar experiments were conducted on two to three anterior segments

returned to near control values after DIDS was removed from the bath (Strange, 1983).

Rapid removal of CO_2 and HCO_3^- from the bath and replacement with a 5.0 mM HEPES-buffered saline caused a rapid and large 30- to 40-mV depolarization of V_{te} (Fig. 7). This depolarization was complete within 1 min ($V_{te} = -12 \pm 1.7$, mean $\pm$ SE, $n = 6$; Fig. 7; see also Fig. 10) and was then followed by a partial repolarization of variable time course (see Strange, 1983). After anywhere from 10 to 90 min, V_{te} stabilized at a new mean value of -31.0 ± 1.1 mV ($\pm$ SE, $n = 6$) which was significantly lower ($P < 0.0005$) than the control V_{te} of -44.6 ± 1.1 mV (mean $\pm$ SE, $n = 6$; Fig. 7). The nature of this repolarization phase is uncertain, but it does not appear to be due to entry of CO_2 from the luminal perfusate into the cell and continued electrogenic HCO_3^- secretion. Removal of luminal CO_2 and HCO_3^- and replacement with HEPES saline causes only a very small 1- to 3-mV hyperpolariza-

tion of V_{te} (mean $\pm$ SE hyperpolarization $= 1.8 \pm 0.3$ mV; $n = 4$) irrespective of the presence or absence of CO_2 and HCO_3^- in the serosal medium.

Replacement of CO_2 and HCO_3^- with the lipid-soluble buffer, glycodiazine, caused V_{te} to rapidly depolarize and to reverse (i.e. lumen positive; Fig. 7). This new positive V_{te} of 2.2 ± 2.6 mV (mean $\pm$ SE, $n = 3$) remained stable for at least 60 min ($V_{te} = 1.4 \pm 1.2$ mV after 60 min; mean $\pm$ SE, $n = 3$). Addition of CO_2 and HCO_3^- back to the bath caused V_{te} to repolarize rapidly and usually hyperpolarize by 5 to 10 mV (Fig. 9).

To determine at which cell membrane these 20- to 50-mV changes in V_{te} were occurring, the experiments with acetazolamide, HEPES and glycodiazine were repeated while simultaneously measuring V_{bl}. Addition of acetazolamide to the bath, or replacement of serosal CO_2 and HCO_3^- with glycodiazine, caused V_{bl} to hyperpolarize slightly by 1 to 3 mV (Figs. 8 and 9). Replacement of CO_2 and
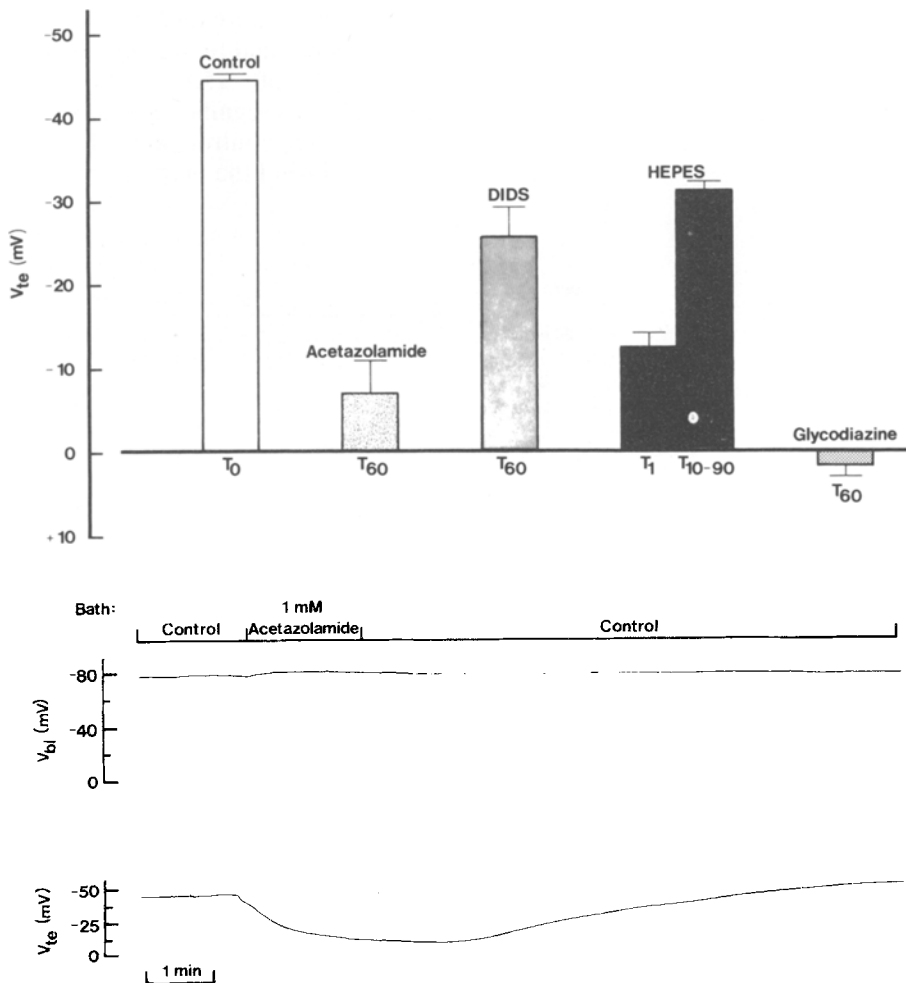

Fig. 7. Transepithelial potentials recorded across anterior segments under control conditions, during addition of 1.0 mM acetazolamide or 0.5 mM DIDS to the bath, or during replacement of serosal CO_2 and HCO_3^- with a HEPES- or glycodiazine-buffered saline. The T-values on the horizontal axis represent the time (in minutes) after the experimental perturbation at which these potentials were recorded. Values are means $\pm$ SE ($n = 4$ to 39)

Fig. 8. Transepithelial potential (V_{te}) and basolateral membrane potential (V_{bl}) during and after addition of 1.0 mM acetazolamide to the serosal bathing saline. A total of 12 similar experiments were conducted on four separate anterior segment preparations with similar results

HCO_3^- with HEPES causes a small, transient (2 to 4 mV) depolarization of V_{bl} (Fig. 10). Rapid increases of serosal HCO_3^- concentration from 18.5 to 65 or 113 mM at constant pH caused V_{bl} to depolarize slightly by 2 to 4 mV and had a small hyperpolarizing effect of 3 to 4 mV on V_{te} (Strange, 1983). Taken together these results indicate that the basolateral membrane has a negligible HCO_3^- conductance and suggest that HCO_3^- movement across the apical membrane is mediated by an electrogenic transport mechanism. In summary, all perturbations which inhibit net total CO_2 secretion and which also cause large (20 to 50 mV) depolarizations of V_{te} are associated with large hyperpolarizations of V_a without significant changes in V_{bl}. These results are all consistent with reduction in net electrogenic exit of HCO_3^- from cell to lumen (or its functional equivalent).

It must be stressed here that the effects of serosal CO_2 and HCO_3^- removal or acetazolamide addition on V_a cannot be explained by an indirect inhibitory action of changes in pH_c on an apical electrogenic cation reabsorptive process. Data in Fig. 4 indicate that the apical membrane already has a negligible cation conductance under control conditions. Conversely, to attribute the large changes in V_a caused by HCO_3^- and CO_2 removal to increases in cell to lumen Na^+ and K^+ conductances would require intracellular activities of 800 to 2500 mM and 270 to 800 mM, respectively, for these cations. This is clearly unrealistic, especially considering that data in Fig. 5 suggest an intracellular K^+ of 120 to 130 mM. Similarly, the observed large alterations in V_a cannot be due to an increased apical Cl^- conductance arising from changes in pH_c. Perfusion of the lumen with Cl^--free saline followed by removal of CO_2 and HCO_3^- from the serosal bath has

the same hyperpolarizing effect on V_a as was observed after CO_2 and HCO_3^- removal from glands perfused with control salines (compare Fig. 11 with Fig. 10). Clearly, HCO_3^- and CO_2 removal causes apical hyperpolarization even when the net driving force for Cl^- movement across the apical membrane is reversed.

Discussion

Previous studies have shown that HCO_3^- secretion in the anterior rectal salt gland of *Aedes dorsalis* is mediated by a 1 : 1 exchange of luminal Cl^- for serosal HCO_3^- ions (Strange & Phillips, 1984; Strange et al., 1984). In the present study we have examined the cellular mechanisms of HCO_3^- secretion and Cl^- reabsorption using conventional ion- and voltage-sensitive microelectrodes. Data in Figs. 7 to 10 show clearly that experimental conditions which inhibit $J_{net}^{CO_2}$ in this tissue (*see* Strange & Phillips, 1984) cause 20- to 50-mV hyperpolarizations of V_a and have little effect on V_{bl}, suggesting an apical electrogenic HCO_3^- or H^+/OH^- transport step. At present it does not appear that this transport mechanism is a simple HCO_3^- conductance since complete removal of mucosal CO_2 and HCO_3^- has little effect on V_{te} (*see* Results). Furthermore, it is unlikely that the apical transporter represents an H^+ or OH^- conductance pathway. Removal of serosal CO_2 and HCO_3^- causes an intracellular alkalinization of *ca.* 0.5 pH units in anterior rectal cells (Strange, 1983) which should increase the gradient for conductive H^+ entry or OH^- exit causing depolarization of V_a rather than the observed hyperpolarization. While further studies are required to clarify this point, we tentatively suggest that HCO_3^- secretion or the equivalent process is mediated by an electrogenic
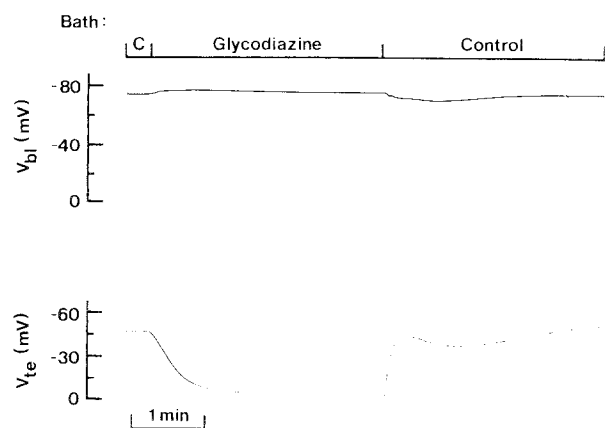
Fig. 9. Effects of serosal CO_2 and HCO_3^- replacement with the lipid-soluble buffer, glycodiazine, on V_{bl} and V_{te}. Eight similar experiments were conducted on three separate anterior segment preparations with similar results
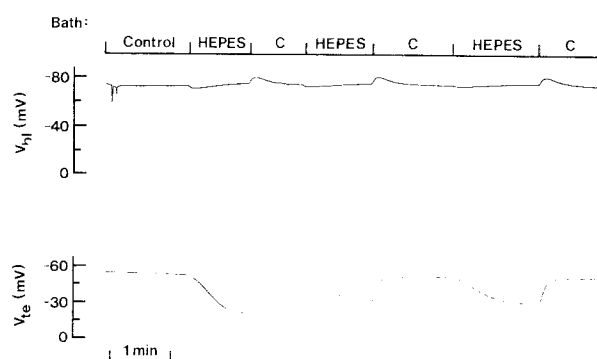
Fig. 10. Effects of replacement of serosal CO_2 and HCO_3^- with a 5.0 mM HEPES-buffered saline on V_{bl} and V_{te}. Seventeen similar experiments were performed on five separate anterior segment preparations with similar results
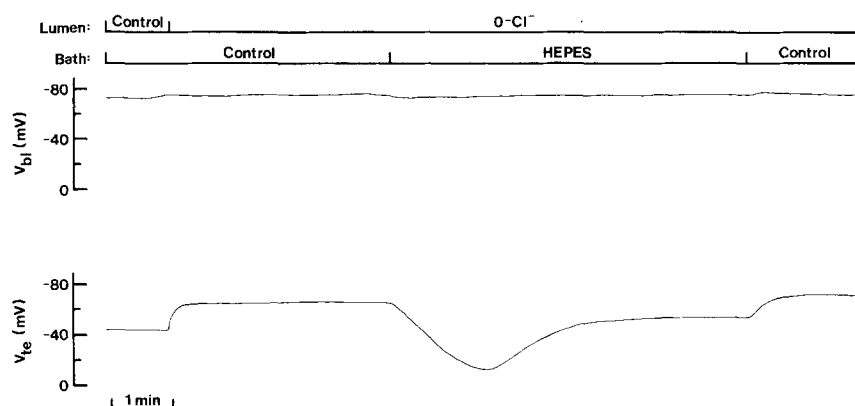
Fig. 11. Effects of serosal CO_2 and HCO_3^- removal (replaced with HEPES-buffered saline) on V_{bl} and V_{te} during perfusion of the anterior segment with Cl^--free salines. Seven similar experiments were conducted on four anterior segment preparations

carrier mechanism located in the apical cell membrane.

Recently, Biagi et al. (1981) have shown that decreases in serosal HCO_3^- concentration and pH depolarize V_{bl} and inhibit basolateral K^+ conductance in perfused rabbit proximal tubules (*see also* Steels & Boulpaep, 1976). These changes in K^+ conductance are presumably due to effects of changes in pH_c on basolateral K^+ channels and could suggest falsely a high HCO_3^- permeability of the basolateral cell membrane. Similar effects cannot explain the results in Figs. 7 to 10. Rapid changes in, or complete removal of, luminal Na^+ or K^+ have little effect on V_a, demonstrating that the apical membrane has a very low cation permeability (Fig. 4). In addition, the alterations of V_a seen in Figs. 8 to 10 are not due to increasing apical Cl^- conductance. Removal of CO_2 and HCO_3^- from the bath still causes a large depolarization of V_{te} when salt glands are perfused with Cl^--free saline (Fig. 11).

Decreases in luminal Cl^- concentration from 164 to 16 mM depolarizes V_a in a rapid, step-wise manner (Fig. 2). The relationship between V_a and luminal Cl^- activity is linear with a slope of 42.2 mV/decalog $a_{Cl^-}^l$ (Fig. 3) indicating that the apical membrane has a very high passive Cl^- conductance. At luminal Cl^- concentrations below 16 mM, V_a begins to repolarize. Mean V_a in the presence of 4 mM luminal Cl^- was close to 0 mV (*see* Fig. 3). The nature of this repolarization phase is uncertain, but it may be due to an inhibitory effect of low luminal Cl^- concentration on electrogenic HCO_3^- secretion (*see* Strange et al., 1984).

Intracellular Cl^- activity in anterior rectal cells was 23.5 mM (Table 2). The calculated $\Delta\bar{\mu}Cl^-/F$ at the apical membrane was -10.7 ± 2.2 mV favoring passive entry of Cl^- from lumen to cell. Taken together, these results suggest strongly that apical Cl^-

entry is mediated, at least in part, by passive, electrodiffusive movement of Cl^- through a Cl^- selective channel.

Intracellular Cl^- measurements in tissues and cells bathed for prolonged periods in Cl^--free salines give "apparent" $a_{Cl^-}^c$ values of 4 to 6 mM (e.g. Spring & Kimura, 1978; Baumgarten & Fozzard, 1981). This residual Cl^- activity is thought to be due to the presence of interfering anions in the cell and most measurements of $a_{Cl^-}^c$ are assumed to be overestimates of actual values. No attempt was made in the present study to measure this residual anion activity primarily because it was anticipated that the concentration of the major intracellular interfering anion, HCO_3^-, would be altered by removing luminal and bath Cl^-. It must be stressed, however, that any overestimate of $a_{Cl^-}^c$ by as much as 6 mM, as discussed above, would only increase the favorable driving force for passive Cl^- entry from 10.7 to 16.7 mV.

Attempts to study the effects of ion transport inhibitors on apical entry and exit steps were not possible. The insect hindgut epithelium is lined by a layer of cuticle which contains pores with a radius of *ca.* 6.5 Å (Phillips & Dockrill, 1968; Lewis, 1971). This cuticle functions as a molecular sieve preventing large molecules (mol wt >200) from interacting directly with the apical membrane. Previous attempts to remove this cuticle using a variety of treatments were unsuccessful (Strange & Phillips, 1984).

Chloride exit from the cell at the basolateral membrane is electrically silent. Figure 6 shows the results of three separate experiments in which serosal Cl^- concentration was varied rapidly from a control value of 39 mM to values of 5, 100 or 164 mM. These solution changes had virtually no effect on V_{bl}. The small potential changes which did occur, and which are seen most easily in the lower

trace of Fig. 6, are clearly in the wrong direction to be explained by an electrogenic, basolateral Cl^- exit step.

Basolateral HCO_3^- entry also appears to be an electrically silent process. Increasing bath HCO_3^- concentration (*see* Results) or complete removal of serosal CO_2 and HCO_3^- (Figs. 9 to 11; *see also* Fig. 8) have little effect on V_{bl}. These results, plus the fact that the Cl^-/HCO_3^- exchange inhibitor DIDS inhibits $J_{net}^{CO_2}$ in this tissue (Strange & Phillips, 1984) and depolarizes V_{te} when added to the serosal bath (Fig. 7) suggest strongly that the basolateral membrane is the site of the putative Cl^-/HCO_3^- exchanger which mediates transepithelial HCO_3^- and Cl^- transport (Strange et al., 1984).

In the present study, cellular HCO_3^- concentration was calculated from measurements of pH_c using the Henderson-Hasselbalch equation and by assuming that pCO_2, K_1', CO_2 solubility coefficients, and HCO_3^- activity coefficients were the same inside the cell as in free solution. It is uncertain whether these assumptions actually hold *in vivo*. At present, however, calculation of HCO_3^- concentration provides the best means of estimating intracellular HCO_3^- activity. Given the above assumptions it follows that $-\Delta\bar{\mu}_{H+} = \Delta\bar{\mu}_{HCO_3^-}$.

Table 2 shows the calculated $\Delta\bar{\mu}_{HCO_3^-}$ for apical and basolateral cell membranes under control conditions. Bicarbonate entry into the cell, or the equivalent process at the serosal membrane, is against an unfavorable electrochemical gradient of 77.1 mV and therefore must be mediated by an active transport process. It is uncertain at present, however, whether the Cl^-/HCO_3^- exchanger is a primary (ATP-driven) pump, or whether it is a secondary active transport process, whereby the basolateral Cl^- electrochemical gradient of 71.7 mV (Table 2) favoring Cl^- exit energizes active, basolateral HCO_3^- entry. Assuming that $a_{Cl^-}^c$ may be overestimated by 4 to 6 mM as discussed above, then $\Delta\bar{\mu}_{Cl^-}^{bl}$ decreases from 71.7 (Table 2) to 64.3 − 67 mV, so that less energy would be available in the Cl^- gradient to drive HCO_3^- accumulation (against 77 mV); i.e. such a Cl^- measurement error would favor a primary exchange mechanism. Even if the overestimation of $a_{Cl^-}^c$ which is inherent in microelectrode measurements is ignored, and it is assumed that there is 100% coupling efficiency between Cl^- and HCO_3^- movements, there still does not appear to be sufficient energy stored in the $\Delta\bar{\mu}_{Cl^-}^{bl}$ to drive HCO_3^- into the cell. If the transporter is indeed a 1 : 1 electroneutral exchanger, then only the chemical gradients should be involved in calculation of net driving forces. Here again, there may not be an adequate chemical gradient to drive the exchange. For exam-

ple, Cl^- exits the cell against a chemical difference of at least 5 mM (or up to 11 mM if one assumes an intracellular Cl^- measurement error of 6 mM; serosal Cl^- activity is 28.5 mM), while HCO_3^- enters against an insignificant chemical difference of approximately 1 mM (external HCO_3^- activity of 13.5 mM). Given experimental errors and these small chemical gradients, it would be premature to conclude whether such a neutral process is either secondary or primary transport.

Under control conditions, HCO_3^- exit at the apical cell membrane is down a favorable electrochemical gradient of 27.6 mV (Table 2). These experiments alone do not demonstrate that apical HCO_3^- transport is normally a downhill process and further studies are needed to determine if $\Delta\bar{\mu}_{HCO_3^-}^a$ favors passive HCO_3^- movement under a variety of experimental conditions.

Data in Fig. 5 indicate that the anterior rectal cell V_{bl} is primarily a K^+ diffusion potential. Changes in serosal K^+ concentration alter V_{bl} in a rapid, linear fashion. The slope of the relationship between V_{bl} and serosal K^+ activity (a_{K+}^s) was 54.2 mV/decalog a_{K+}^s with a correlation coefficient of 0.9999.

The nature of the K^+ uptake mechanism across the basolateral membrane of anterior rectal cells is uncertain at present. Superfusion of the tissue with 1.0 mM serosal ouabain for up to 1 hr had no effect on V_{bl} or V_{te} (*data not shown*). This may be due to an insensitivity of a putative Na^+, K^+-ATPase to ouabain at room temperature as observed for other insect Na^+/K^+ pumps (reviewed by Anstee & Bowler, 1979). Alternatively, it could simply represent failure of the ouabain to permeate the basement membrane and very long basal infoldings so as to interact with pump sites. Since Na^+/K^+ pumps have been found in a number of insect tissues (*see* Anstee & Bowler, 1979; Phillips, 1981) and are present in almost all vertebrate epithelia studied in detail, it is tentatively suggested that anterior rectal cell K^+ accumulation is mediated by a basolateral Na^+, K^+-ATPase. These and the results above are summarized in the tentative cellular model shown in Fig. 12.

It must be stressed here that the actual species (i.e. HCO_3^-, H^+, or OH^-) involved in transepithelial HCO_3^- secretion are not known. Experiments using glycodiazine suggest, albeit *very indirectly*, that basolateral Cl^- exit and HCO_3^- entry may at least partially be mediated by an HCl cotransport or Cl^-/OH^- exchange mechanism. Glycodiazine (sodium glymidine) is a buffer which has a high lipid solubility. The pK_a of glycodiazine (5.7; Ullrich, Radtke & Rumrich, 1971) is similar to that for the CO_2/HCO_3^-
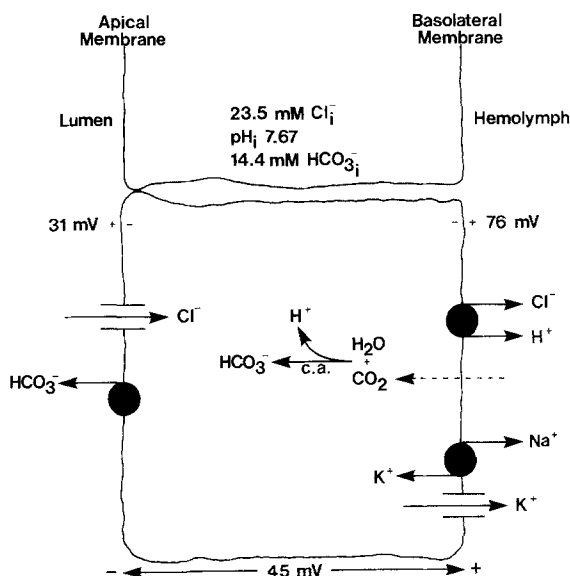
Fig. 12. Tentative cellular model of HCO_3^- and Cl^- entry and exit steps in anterior rectal salt gland cells (c.a. = carbonic anhydrase). Note that the actual species (i.e. HCO_3^-, H^+ or OH^-) involved in transepithelial HCO_3^- secretion are not known with certainty (*see* Discussion)

equilibrium (6.1) and hence this compound has been used as a CO_2 and HCO_3^- replacement. In the proximal tubule, it has been shown that glycodiazine is reabsorbed from the tubule lumen at a rate equal to the rate of H^+ secretion (Malnic et al., 1980). Ullrich et al. (1971) have shown that glycodiazine supports normal isotonic fluid reabsorption in the proximal tubule in the absence of ambient CO_2 and HCO_3^-. Furthermore, renal glycodiazine transport displays many characteristics similar to those of H^+ transport, such as Na^+ dependence, inhibitor sensitivity and adaptation to chronic alkalosis (Ullrich, Rumrich & Baumann, 1975). In the pancreas, glycodiazine partially stimulates fluid and solute secretion in the absence of exogenous CO_2 and HCO_3^- (Schulz, 1981). Since the large glycodiazine molecule (mol wt 308) *per se* is unlikely to be transported on a membrane carrier, the experiments on the proximal tubule and pancreas have been taken as evidence that a H^+/OH^- transporter rather than a HCO_3^- carrier is involved in transepithelial acid-base movements. For example, in the proximal tubule, reabsorption of HCO_3^- or the glycodiazine anion is dependent upon tubular H^+ secretion and buffer titration followed by passive diffusion of uncharged CO_2 and H_2CO_3 or glycodiazine molecules from lumen to serosa.

In this and earlier studies we made no attempt to investigate glycodiazine transport *per se* primarily because of the difficulty of obtaining radioac-

tively labeled forms of this compound. The effects of glycodiazine on anterior rectal cell electrophysiology were, however, examined. When CO_2 and HCO_3^- are removed from the serosal saline and replaced with glycodiazine, V_{te} rapidly depolarizes and reverses, and the small positive V_{te} remains stable for at least 60 min (Fig. 7). This positive potential is consistent with the fact that glycodiazine maintains a small component of electrogenic Cl^- reabsorption in the absence of exogenous CO_2 (Strange, 1983), whereas a phosphate or HEPES-buffered saline completely inhibits Cl^- transport in the anterior rectal salt gland (Strange et al., 1984).

In order for glycodiazine to support Cl^- reabsorption in the anterior salt gland, it is necessary to postulate that this compound shuttles protons across the basolateral membrane (*see* Strange, 1983, for a more detailed discussion) in a manner similar to that proposed for a variety of other weak acids (*see* for example McLaughlin & Dilger, 1980; Boron, 1983). Intracellular H^+ could then either be cotransported out of the cell with Cl^- or serve to buffer intracellular OH^- brought into the cell via a Cl^-/OH^- exchanger.

In summary, we tentatively suggest that Cl^- enters the apical cell membrane of the anterior salt gland, at least in part, by passive, electrodiffusive movement through a Cl^--selective pathway, and HCO_3^- exits the cell by an active or passive electrogenic transport mechanism. The basolateral cell membrane is the site of direct coupling between Cl^- and HCO_3^- movements via a Cl^-/HCO_3^- or Cl^-/OH^- exchange or HCl cotransport mechanism. Two important areas which warrant further study in this epithelium and which are currently under investigation are the nature and control of the luminal Cl^- entry step or putative Cl^- channel, and the mechanisms by which the cells of this epithelium regulate their intracellular acid-base balance while simultaneously maintaining a large transcellular CO_2 flux and generating remarkable transepithelial HCO_3^- and CO_3^{2-} gradients.

References

Ammann, D., Lanter, F., Steiner, R.A., Schulthess, P., Shijo, Y., Simon, W. 1981. Neutral carrier based hydrogen ion selective microelectrode for extra- and intracellular studies. *Anal. Chem.* **53:**2267–2269

Anstee, J.H., Bowler, K. 1979. Ouabain-sensitivity of insect epithelial tissue. *Comp. Biochem. Physiol.* **62A:**763–769

Baumgarten, C.M., Fozzard, H.A. 1981. Intracellular chloride activity in mammalian ventricular muscle. *Am. J. Physiol.* **241:**C121–C129

Biagi, B., Kubota, T., Sohtell, M., Giebisch, G. 1981. Intracellular potentials in rabbit proximal tubules perfused *in vitro. Am. J. Physiol.* **240**:F200–F210

Boron, W.F. 1983. Transport of H^- and of ionic weak acids and bases. *J. Membrane Biol.* **72**:1–16

Bradley, T.J., Phillips, J.E. 1975. The secretion of hyperosmotic fluid by the rectum of a saline-water mosquito larva. *Aedes taeniorhynchus. J. Exp. Biol.* **63**:331–342

Brown, H.M., Saunders, J.H. 1977. Cation and anion sequences in dark-adapted *Balanus* photoreceptors. *J. Gen. Physiol.* **70**:531–543

Fujimoto, M., Kubota, T. 1976. Physiochemical properties of a liquid ion exchanger microelectrode and its application to biological fluid. *Jpn. J. Physiol.* **26**:631–650

Kielland, J. 1937. Individual activity coefficients of ions in aqueous solutions. *J. Am. Chem. Soc.* **59**:1675–1678

Lewis, S.A. 1971. Charge properties and ion selectivity of the rectal intima of the desert locust. M.Sc. Thesis, University of British Columbia, Vancouver, B.C.

Malnic, G., Costasilva, V.L., Campiglia, S.S., Mello Aires, M. de, Giebisch, G. 1980. Tubular permeability to buffer components as a determinant of net H^+ ion fluxes. *In:* "Current Topics in Membranes and Transport. Vol. 13: Cellular Mechanisms of Renal Tubular Ion Transport. pp. 257–264. E.L. Boulpaep, editor. Academic Press, New York

McLaughlin, S.G.A., Dilger, J.P. 1980. Transport of protons across membranes by weak acids. *Physiol. Rev.* **60**:825–863

Meredith, J., Phillips, J.E. 1973. Rectal ultrastructure in salt- and freshwater mosquito larvae in relation to physiological state. *Z. Zellforsch.* **138**:1–22

Ogden, T.E., Citron, M.C., Pierantoni, R. 1978. The jet stream microelectrode beveler: An inexpensive way to bevel ultrafine glass micropipettes. *Science* **200**:469–470

Phillips, J. 1981. Comparative physiology of insect renal function. *Am. J. Physiol.* **241**:R241–R257

Phillips, J.E., Bradley, T.J., Maddrell, S.H.P. 1978. Mechanisms of ionic and osmotic regulation in saline-water mosquito larva. *In:* Comparative Physiology—Water, Ions and Fluid Mechanics. K. Schmidt-Nielsen, C. Bollis and S.H.P. Maddrell, editors. pp. 151–171. Cambridge University Press, Cambridge

Phillips, J.E., Dockrill, A.A. 1968. Molecular sieving of hydrophilic molecules by the rectal intima of the desert locust (*Schistocerca gregaria*). *J. Exp. Biol.* **48**:521–532

Phillips, J.E., Maddrell, S.H.P. 1974. Active transport of magnesium by the Malpighian tubules of the larvae of the mosquito *Aedes campestris. J. Exp. Biol.* **61**:761–771

Robinson, R.A., Stokes, R.H. 1965. Electrolyte Solutions. 3rd ed. Buttersworth, London

Schulz, I. 1981. Electrolyte and fluid secretion in the exocrine pancreas. *In:* Physiology of the Gastrointestinal Tract. L.R. Johnson, editor. Vol. 2, pp. 795–819. Raven, New York

Scudder, G.G.E. 1969. The fauna of saline lakes on the Fraser Plateau in British Columbia. *Verh. Int. Ver. Limnol.* **17**:430–439

Spring, K.R., Kumura, G. 1978. Chloride reabsorption by renal proximal tubules of *Necturus. J. Membrane Biol.* **38**:233–254

Steels, P.S., Boulpaep, E.L. 1976. Effect of pH on ionic conductances of the proximal tubule epithelium of *Necturus* and the role of buffer permeability. *Fed. Proc.* **35**:465

Strange, K. 1983. Cellular mechanism of bicarbonate regulation and excretion in an insect inhabiting extreme alkalinity. Ph.D. Thesis, University of British Columbia, Vancouver, B.C.

Strange, K., Phillips, J.E. 1984. Mechanisms of total CO_2 transport in the microperfused rectal salt gland of *Aedes dorsalis*. I. Ionic requirements of total CO_2 secretion. *Am. J. Physiol.* **246**:R727–R734

Strange, K., Phillips, J.E., Quamme, G.A. 1982. Active HCO_3^- secretion in the rectal salt gland of a mosquito larva inhabiting $NaHCO_3$–CO_3 lakes. *J. Exp. Biol.* **101**:171–186

Strange, K., Phillips, J.E., Quamme, G.A. 1984. Mechanisms of total CO_2 transport in the microperfused rectal salt gland of *Aedes dorsalis*. II. Site of Cl^-/HCO_3^- exchange and function of anterior and posterior salt gland segments. *Am. J. Physiol.* **246**:R735–R740

Ullrich, K.J., Radtke, H.W., Rumrich, G. 1971. The role of bicarbonate and other buffers on isotonic fluid absorption in the proximal convolution of the rat kidney. *Pfluegers Arch.* **330**:149–161

Ullrich, K.J., Rumrich, G., Baumann, K. 1975. Renal proximal tubular buffer-(glycodiazine) transport. Inhomogenicity of local transport rate, dependence on sodium, effect of inhibitors and chronic adaptation. *Pfluegers Arch.* **357**:149–163